Hindawi Publishing Corporation
International Journal of Rotating Machinery
Volume 2008, Article ID 784749, 10 pages
doi:10.1155/2008/784749

Research Article

The Fisher Information Matrix as a Relevant Tool for Sensor Selection in Engine Health Monitoring

S. Borguet and O. Léonard

Turbomachinery Group, University of Liège, Chemin des Chevreuils 1, 4000 Liège, Belgium

Correspondence should be addressed to S. Borguet, s.borguet@ulg.ac.be

Received 24 April 2008; Accepted 22 August 2008

Recommended by Eric Maslen

Engine health monitoring has been an area of intensive research for many years. Numerous methods have been developed with the goal of determining a faithful picture of the engine condition. On the other hand, the issue of sensor selection allowing an efficient diagnosis has received less attention from the community. The present contribution revisits the problem of sensor selection for engine performance monitoring within the scope of information theory. To this end, a metric that integrates the essential elements of the sensor selection problem is defined from the Fisher information matrix. An example application consisting in a commercial turbofan engine illustrates the enhancement that can be expected from a wise selection of the sensor set.

1. INTRODUCTION

In the last years, condition-based maintenance has been widely promoted in the jet engine community. A maintenance schedule adapted to the level of deterioration of the engine leads to many advantages such as improved operability and safety or reduced life cycle costs. In this framework, generating a reliable information about the health condition of the engine is a requisite.

In this contribution, module performance analysis, also known as *gas path analysis*, is considered. Its purpose is to assess the changes in engine module performance on the basis of measurements collected along the gas path of the engine [1]. This approach allows to track the evolution of a particular engine relative to some baseline performance which may be engine specific or fleet averaged. The gas path analysis approach is illustrated in Figure 1 and is governed by the following principles:

(i) the condition of the components (e.g., fan, lpc, hpc, hpt, lpt, nozzle) can be represented by a set of performance indicators, so-called *health parameters* $\mathbf{w}$, which are typically correcting factors on their efficiency and flow capacity;

(ii) a degradation (progressive or accidental) affecting the engine induces a modification of its performance, which results in a drift of some *measurements* $\mathbf{y}$ collected along the engine flow path (e.g., temperatures, pressures, mass flows, shaft speeds);

(iii) a *physical or mathematical model*, of the engine that relates the variation of the health parameters $\mathbf{w}$ to the drift of the gas-path measurements $\mathbf{y}$ can be derived.

As depicted in Figure 1, the diagnosis problem (or health parameter estimation problem) can be considered as the inverse problem of performance simulation. Mathematically speaking, the health parameters are estimated by minimising a cost function $\rho(\cdot)$ of the residuals defined as the difference between the measured value $\mathbf{y}$ and the model prediction $\hat{\mathbf{y}}_{\mathbf{w}}$:

$$\hat{\mathbf{w}} = \arg\min_{\mathbf{w}} \{\rho(\mathbf{y} - \hat{\mathbf{y}}_{\mathbf{w}})\}. \tag{1}$$

Next to the definition of the cost function and the choice of an appropriate method to solve the inverse problem, which has been an area of intensive research (see [2] for a detailed review), the selection of a relevant configuration of the sensors is an important issue. Current sensors remain intrusive, their integration is limited by many constraints such as cost, weight, or harsh environment. As a consequence, the number of sensors is usually kept to a minimum and hence outweighed by the number of health parameters. This makes the

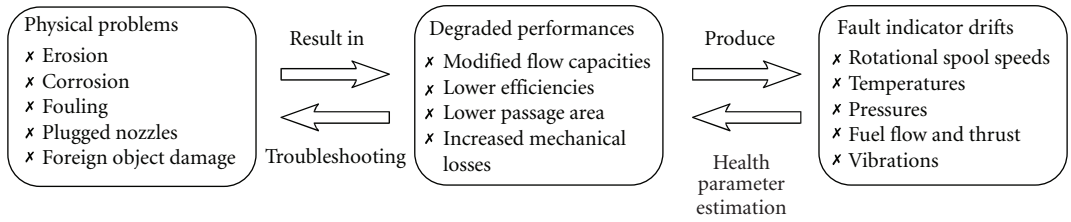

Figure 1: The gas path analysis approach to jet engine diagnostics.

estimation problem ill posed. Moreover, the measurements are corrupted with noise. The efficiency of the diagnosis algorithm depends on the sensor configuration which should therefore be selected so as to optimise the amount of information that is carried about the engine condition.

Optimal sensor selection has been investigated only sparsely in the engine health monitoring community, few contributions indeed address this issue. Most of the work so far is based on linear approaches. In [3], a metric based on the sensitivity of the sensors with respect to the parameters is defined. The use of the condition number of the influence coefficient matrix that relates measurements and parameters is also investigated in order to perform the sensor selection in the case of a square problem (i.e., as many sensors as parameters). In [4], a figure of merit based on the steady-state error covariance matrix of a Kalman filter is used to perform the optimisation of the sensor set, again in the case of a square problem. This study also takes into account the cost of the different sensors. In [5], the strong link between sensor selection and observability is underlined. A sensor configuration is considered as informative if it avoids both redundancy between measurements and correlation between fault directions. The solution of the sensor selection problem relies on a method for observability analysis developed in [6].

The same topic has received much more attention in other fields such as chemical or structural engineering. As a general trend (see for instance [7–10]), the sensor selection problem is addressed in the framework of information theory. Metrics based on the observability Grammian or on the Fisher information matrix are defined in order to optimise the configuration of the experiment.

In the light of these considerations, the present contribution revisits the problem of sensor selection for turbine engine performance monitoring within the scope of information theory. The application consists in a generic turbofan model developed in the frame of the European OBIDICOTE project. A metric that handles the aforementioned particularities is proposed. With the research being focused on the metric definition itself, the optimal configuration is obtained through a brute-force technique. The quality of the resulting sensor set is assessed on the basis of fault cases that can be expected on a turbofan engine, and an observability analysis is performed to get more knowledge about the sensor configuration.

2. STATEMENT OF THE PROBLEM

The scope of this section is to present the theoretical foundation of the methodology developed for sensor selection. First, the model relating the observations to the parameters is described. Elements of information theory are then introduced in the scope of sensor selection, with a particular focus on the Fisher information matrix (FIM). Metrics based on the FIM are subsequently proposed in order to optimise the measurement configuration for a given set of health parameters. Finally, guidelines to perform an observability analysis of a given configuration are proposed.

2.1. Simulation model

One of the master pieces of the gas path analysis approach is a simulation model of the engine. Considering steady-state operation of the engine, these simulation tools are generally nonlinear aerothermodynamic models based on mass, energy, and momentum conservation laws applied to the engine flow path. Equation (2) represents such an engine model where $\mathbf{u}$ are the variables defining the operating point of the engine (e.g., fuel flow, altitude, Mach number), $\mathbf{w}$ are the aforementioned health parameters, and $\mathbf{y}$ are the gas path measurements:

$$\mathbf{y} = \mathcal{G}(\mathbf{u}, \mathbf{w}). \tag{2}$$

In the frame of turbine engine diagnosis, the statistical model is rarely used in the previous form stated by (2). Indeed, the quantity of interest is the difference between the actual engine health condition and a reference one represented by baseline values $\mathbf{w}^{bl}$. Assuming a linear relationship between the measurements and the health parameters, as well as fixed operating conditions, the model is re-formulated according to

$$\mathbf{y} = \mathbf{y}^{bl} + \mathbf{G}\,(\mathbf{w} - \mathbf{w}^{bl}) \iff \delta\mathbf{y} = \mathbf{G}\,\delta\mathbf{w}, \tag{3}$$

where

$$\mathbf{y}^{bl} = \mathcal{G}(\mathbf{u}, \mathbf{w}^{bl}), \qquad \mathbf{G} = \frac{\partial}{\partial \mathbf{w}} \mathcal{G}(\mathbf{u}, \mathbf{w}) \bigg|_{\mathbf{w}=\mathbf{w}^{bl}} \tag{4}$$

are, respectively, the prediction of the measurements and the Jacobian matrix of the engine model around the baseline $\mathbf{w}^{bl}$.

A random variable $\boldsymbol{\epsilon} \in \mathcal{N}(\mathbf{0}, \mathbf{R}_{\mathbf{y}})$ which accounts for sensor inaccuracies and modelling errors is added to the deterministic linearised model (3) in order to reconcile the observed measurements and the model predictions. Equation (5) is therefore termed the statistical model:

$$\delta\mathbf{y} = \mathbf{G}\,\delta\mathbf{w} + \boldsymbol{\epsilon}. \tag{5}$$

The statistical model (5) can further be scaled to a linear system with a noise distribution $\tilde{\boldsymbol{\epsilon}} \in \mathcal{N}(\mathbf{0}, \mathbf{I})$ provided that the covariance matrix $\mathbf{R}_\mathbf{y}$ is positive definite. The scaled model is given by $\tilde{\mathbf{G}} = (\sqrt{\mathbf{R}_\mathbf{y}})^{-1}\,\mathbf{G}$, where the scaling factor takes into account the relative accuracy of each sensor.

$$\tilde{\boldsymbol{\epsilon}} = \delta\tilde{\mathbf{y}} - \tilde{\mathbf{G}}\,\delta\mathbf{w}, \tag{6}$$

The scaled statistical model is actually the probability density function of the residuals $\tilde{\boldsymbol{\epsilon}}$ parameterised by the health parameters $\delta\mathbf{w}$:

$$p(\tilde{\boldsymbol{\epsilon}} \mid \delta\mathbf{w}) = \frac{1}{\sqrt{(2\pi)^m}} \exp\left(-\frac{1}{2}\tilde{\boldsymbol{\epsilon}}^T\tilde{\boldsymbol{\epsilon}}\right). \tag{7}$$

2.2. Fisher information matrix

The idea behind sensor selection is to optimise the amount of information conveyed by the measurements about the parameters to be estimated. Optimal information can be defined in various ways, such as maximum response of the measurements to a change in the health condition, minimum uncertainty in the estimated parameters, or maximum orthogonality between the measurements to name a few. This question will be addressed in more details in the next section. It is desirable to base the optimisation on a quantity that captures these properties and that allows easy comparison between different configurations.

For the kind of static systems described by (6), the Fisher information matrix (FIM) is a mathematical entity that possesses the aforementioned features. Indeed, the FIM quantifies the amount of information that an observation carries about an unknown parameter. Mathematically, the FIM is defined as the variance of the score function associated to the estimation problem [11]. Loosely speaking, it is intimately linked to the sensitivity of the measurements with respect to the parameters.

Considering the joint probability distribution of the residuals and the parameters $p(\tilde{\boldsymbol{\epsilon}}, \delta\mathbf{w})$, which characterises the estimation problem, the general term of the FIM is defined as

$$\mathbf{FIM}_{i,j} \overset{\text{def}}{=} E\left\{\frac{\partial}{\partial\delta\mathbf{w}_i}\log p(\tilde{\boldsymbol{\epsilon}}, \delta\mathbf{w}) \cdot \frac{\partial}{\partial\delta\mathbf{w}_j}\log p(\tilde{\boldsymbol{\epsilon}}, \delta\mathbf{w})\right\}, \tag{8}$$

where $E\{\cdot\}$ is the mathematical expectation operator and log, the natural logarithm. The existence of the FIM is conditioned on some regularity assumptions of the probability density. In the following, two cases widely used in practice are studied.

Consider first the estimation of the health parameters in a maximum likelihood (ML) framework. The health parameters are seen in this case as deterministic variables that are assessed from the available measurements. Consequently, the joint probability density function is equal to the probability density function of the residuals conditioned on the health parameters:

$$p_{\text{ML}}(\tilde{\boldsymbol{\epsilon}}, \delta\mathbf{w}) = p(\tilde{\boldsymbol{\epsilon}} \mid \delta\mathbf{w}). \tag{9}$$

Clearly, the Gaussian distribution used to model $p(\tilde{\boldsymbol{\epsilon}} \mid \delta\mathbf{w})$ is such that its natural logarithm as well as its first derivative with respect to the parameters can be computed for any values of these parameters. Substituting expression (7) in relation (8), the FIM writes down:

$$\mathbf{FIM}_{\text{ML}} = \tilde{\mathbf{G}}^T\tilde{\mathbf{G}}. \tag{10}$$

Consider now the Bayesian approach to estimation. Both the measurements and the health parameters are seen as random variables. The joint probability density function is here equal to the product of the probability density function of the residuals conditioned on the health parameters and the a priori probability density function of the health parameters:

$$p_{\text{Bayes}}(\tilde{\boldsymbol{\epsilon}}, \delta\mathbf{w}) = p(\tilde{\boldsymbol{\epsilon}} \mid \delta\mathbf{w}) \cdot p(\delta\mathbf{w}). \tag{11}$$

The prior distribution of the parameters is chosen as $\delta\mathbf{w} = \mathcal{N}(\mathbf{0}, \mathbf{Q})$, where $\mathbf{Q}$ is the prior covariance matrix of the parameters. Moreover, the parameters and the measurements are assumed to be *statistically* independent. Under these hypotheses, the FIM takes the form

$$\mathbf{FIM}_{\text{Bayes}} = \tilde{\mathbf{G}}^T\tilde{\mathbf{G}} + \mathbf{Q}^{-1}. \tag{12}$$

Interestingly, the Cramer-Rao inequality [12] states that the diagonal terms of the inverse of the FIM (provided that it exists) are *asymptotic* lower bounds on the variance of any unbiased estimator of $\delta\mathbf{w}$. This underlines the strong coupling between information, observability, and estimation.

Engine performance monitoring is characterised in practice by negative redundancy, which means that the number of parameters exceeds the number of sensors ($n > m$). In this case, the ML formulation leads to an underdetermined estimation problem that has no unique solution. Bayesian estimation has to be applied as a palliative. As already mentioned, sensor selection relies here on the FIM. Comparing (10) and (12), it can be seen that the FIM in the Bayesian case is equal to the one of the ML case, which effectively depends on the sensor configuration, plus the contribution of the a priori knowledge. This latter term can be interpreted as an additional information that makes the mathematical problem well posed. As a conclusion, the sensor selection problem will be solved by using the FIM of the ML framework, even in the case $m < n$.

2.3. Figures of merit for sensor selection

In the previous section, it has been shown that the FIM is a relevant mathematical entity on which the sensor selection can rely. Practically, two main objectives govern the design of a diagnosis tool. On the one hand, high sensitivity is desirable in order to provide an early detection of a fault. On the other hand, the user's confidence in the system is conditioned by a minimum false alarm rate. These objectives can be achieved by determining the configuration that maximises both the orthogonality between the sensors and the orthogonality between the parameters. The former means that two sensors should not react in the same way to any engine fault. The

latter means that two parameters should have a distinct signature on the observations. Various scalar figures of merit based on the FIM can describe these objectives:

(1) the *condition number* CN of the FIM is defined as the ratio of the largest to the smallest singular value. The condition number is linked to the rank of a matrix and to the difficulty in performing its inversion. In the case $m < n$, the rank of the FIM is at best equal to m which can be ensured by minimising the condition number. In that way, no sensor is redundant with another;

(2) the *trace* Tr of the FIM is defined as the sum of the singular values. In the case $m < n$, the sum is limited to the first m singular values. The trace is a measure of the global sensitivity of the sensors with respect to the parameters and hence has to be maximised. It is linked to some extent to the sensitivity measure defined in [3];

(3) the *determinant* Det of the FIM is defined as the product of the singular values. Again, the product is restricted to the first m singular values. Indeed, as stated in point 1, at most m singular values are nonzero. This quantity has to be maximised too as the inverse of the determinant is a measure of the overall uncertainty on the estimated parameters. Furthermore, this criterion tends to standardise the singular values and hence the contribution of each sensor. This criterion is similar to the one used in [5].

Relations (13) give the mathematical form of the figures of merit, where σ_i, $i = 1, \ldots, m$ are the singular values, see next section for a definition of singular value, of the FIM sorted in descending order:

$$\mathtt{CN} = \frac{\sigma_1}{\sigma_m}, \qquad \mathtt{Tr} = \sum_{i=1}^{m} \sigma_i, \qquad \mathtt{Det} = \prod_{i=1}^{m} \sigma_i. \tag{13}$$

Each of those metrics puts emphasis on a particular aspect of the problem at hand. To perform the sensor selection, it is thus proposed to combine them in an aggregated figure of merit:

$$\mathtt{FOM} = -W_1 \log(\mathtt{CN}) + W_2 \log(\mathtt{Tr}) + W_3 \log(\mathtt{Det}), \tag{14}$$

where W_i are factors that allow both normalisation of the magnitude of the various components and variable weighting between the objectives. For the problem considered in this study, FOM has to be maximised with respect to the sensor configuration under the constraint of a fixed number of sensors.

2.4. Metrics for observability analysis

The purpose of the observability analysis as considered in the present study is twofold: firstly assessing the contribution of each sensor to the estimation problem and secondly quantifying the observability level of each health factor. In simple words, the observability level measures the possibility to estimate correctly a given parameter.

As pointed by Brown in [13], the classical test for observability, that is, checking the invertibility (or full rank) of the system matrix—$\widetilde{\mathbf{G}}$ here—gives merely a boolean answer. In the case of negative redundancy, the system is always classified as nonobservable. Practically, it is however *partially* observable, and it is worth determining the observability level of the different parameters as well as the unobservable fault directions. Inspired by the work of Provost [6], a method for generating this information is proposed in the following.

The intent is to derive metrics for both the sensors and the parameters, the computation is therefore based on the scaled Jacobian matrix rather than on the FIM. Singular value decomposition (SVD) (see [14]) of $\widetilde{\mathbf{G}}$ serves as the mathematical tool to carry out the observability analysis:

$$\widetilde{\mathbf{G}} = \mathbf{U}\,\mathbf{\Sigma}\,\mathbf{V}^T = \mathbf{U}\,[\mathbf{\Sigma}_1\ \mathbf{\Sigma}_2]\,[\mathbf{V}_1\ \mathbf{V}_2]^T, \tag{15}$$

where

(i) $\mathbf{U} \in \mathcal{R}^{m\times m}$ is an orthogonal matrix whose columns define an orthonormal basis for the output (measurement) space;

(ii) $\mathbf{V} \in \mathcal{R}^{n\times n}$ is an orthogonal matrix whose columns define an orthonormal basis for the input (parameter) space;

(iii) $\mathbf{\Sigma} \in \mathcal{R}^{m\times n}$ is a rectangular matrix whose main diagonal contains the singular values σ, which can be seen as stretching factors along the directions defined in $\mathbf{U}$ and $\mathbf{V}$.

A more practical interpretation of the SVD is proposed hereafter. The scaled Jacobian matrix $\widetilde{\mathbf{G}}$ can be seen as an operator that maps the space of the health parameters (input space) to the space of the measurements (output space). In this representation, each health parameter (resp., measurement) is one orthogonal base vector of the input (resp., output) space. Application of the SVD to the matrix consists essentially in a change of reference frame in both the input and output spaces. The position of any health condition of the engine is now measured according to the columns of matrix $\mathbf{V}$, and the corresponding measurement coordinates are expressed in terms of the columns of matrix $\mathbf{U}$. The major difference between the two representations (original and SVD) lies in the mapping from the input space to the output space. In the SVD representation, the mapping is given by the diagonal matrix $\mathbf{\Sigma}$ which simplifies the description of the input-output relation.

Given the meaning of the columns of $\mathbf{U}$ and the diagonal terms of $\mathbf{\Sigma}$, a sensitivity index SI is defined for each sensor as a weighted norm of each row of $\mathbf{U}$:

$$\mathtt{SI}_i = \mathbf{U}_i \sqrt{\mathbf{\Sigma}^T \mathbf{\Sigma}}\, \mathbf{U}_i^T, \quad i = 1, \ldots, m. \tag{16}$$

This sensitivity index is an image of the overall contribution of a given sensor to the estimation process. The higher the SI,

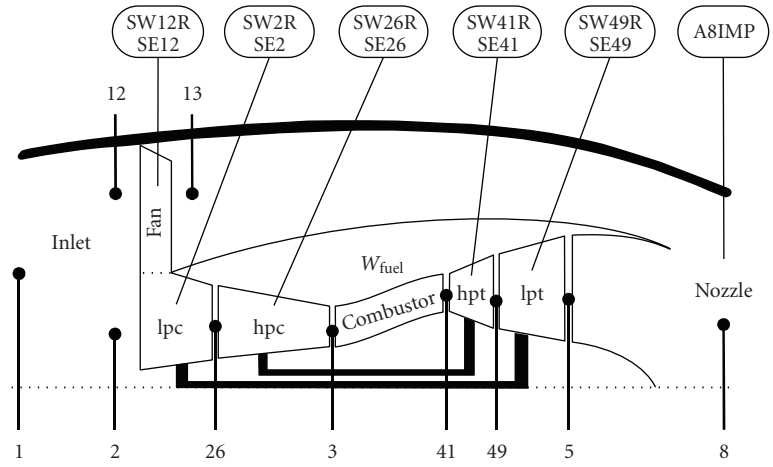

Figure 2: Turbofan layout with health parameters location.

the more important the influence of the associated sensor in the estimation of the health parameters.

An observability index for the parameters, and to a larger extent for any fault (i.e., combination of several parameters), could be defined in a similar way as the sensitivity index is. Nonetheless, in the case of negative redundancy, a loss of information is introduced due to the fact that the number of parameters outweighs the number of sensors. From linear algebra theory, it can be stated that the rank of the Jacobian matrix $\widetilde{\mathbf{G}}$ is at best equal to m. Hence, $n - m$ singular values are equal to zero. As highlighted in the second part of (15), matrix $\boldsymbol{\Sigma}$ is partitioned in two where $\boldsymbol{\Sigma}_1^T$ gathers the m nonzero singular values and $\boldsymbol{\Sigma}_2^T$ is a submatrix containing the $n - m$ null singular values. Matrix $\mathbf{V}$ is accordingly split column-wise into the observable subspace $\mathbf{V}_1$ and its unobservable counterpart $\mathbf{V}_2$, also known as the null space, which does not carry any information about the state of the system [15].

The definition of the observability index proposed in the present study quantifies this loss of information. For some fault $\mathbf{f}$, the observability index $\mathtt{OI}$ is computed according to

$$\mathtt{OI}_{\mathbf{f}} = \frac{\|\mathbf{V}_1^T \mathbf{f}\|^2}{\|\mathbf{V}^T \mathbf{f}\|^2}, \tag{17}$$

where the numerator is a measure of the intensity of fault $\mathbf{f}$ in the observable subspace, and the denominator represents the total intensity of fault $\mathbf{f}$.

Following this definition, the observability index is bounded by zero and one. An observability index equal to unity means that the considered fault has no component located in the null space and can therefore be estimated with a great accuracy. On the contrary, a small observability index characterises a large loss of information. The estimation of the associated fault is hence less accurate.

The fault directions defined by the columns of matrix $\mathbf{V}_2$ are unobservable in the sense that they produce no shift in the measurements. Any fault direction that is a linear combination of these vectors has obviously the same detrimental property. The examination of the unobservable fault directions gives clues about possible confusions between weakly observable faults.

Table 1: Cruise point definition.

Label	W_{fuel}	Altitude	Mach	ΔT_{ISA}
Value	0.350 kg/s	10668 m	0.80	0.0 K

3. APPLICATION OF THE METHOD

3.1. Engine layout

The application considered as a test case is a large bypass ratio, mixed-flow turbofan. The engine performance model was developed in the frame of the OBIDICOTE project, a Brite-Euram project for onboard identification, diagnosis, and control of turbofan engine, and is detailed in [16]. A schematic of the engine is sketched in Figure 2, where the location of the eleven health parameters and the station numbering are also indicated. One control variable is considered in the following, namely, fuel flow rate W_{fuel} fed in the combustor.

The sensor selection problem is formulated for the case of an onboard engine performance monitoring tool. As steady-state operation of the engine is achieved nearly exclusively during the cruise phase, the corresponding operating point is selected for this study. Cruise conditions are defined in Table 1.

Sensors that may be fitted on the engine are listed with their associated uncertainty (noise level) in Table 2. They mostly consist in total temperature and pressure at various intercomponent planes as well as both spool speeds.

3.2. Optimisation of the sensor configuration

The optimisation problem is to determine the m (among twelve) sensors that maximise the figure of merit of (14) for the set of $n = 11$ health parameters depicted in Figure 2 at cruise conditions. The only parameter that still needs to be set is the number of sensors that are installed on the engine.

Table 2: Available sensors (uncertainty is three times the standard deviation).

Label	P13	P26	NLP	P3	P49	*P*5
Uncertainty	±100 Pa	± 500 Pa	±6 rpm	±5000 Pa	±500 Pa	±300 Pa
Label	T13	T26	NHP	T3	T49	T5
Uncertainty	±2 K	±2 K	±12 rpm	±2 K	±2 K	±2 K

Table 3: First ten optimal configurations.

	P13	T13	P26	T26	NLP	NHP	P3	T3	P49	T49	P5	T5	FOM
1	√		√		√	√	√		√	√			−1.4254
2	√		√		√	√		√	√	√			−1.5968
3	√		√		√	√	√	√	√				−1.7014
4	√		√		√	√	√		√			√	−1.7315
5	√		√		√	√		√	√			√	−1.8936
6	√				√	√	√	√	√	√			−2.0492
7	√		√			√	√	√	√	√			−2.1709
8	√		√		√		√	√	√	√			−2.2540
9	√		√		√		√	√	√	√			−2.2576
10			√		√	√	√	√	√	√			−2.2819
	9	0	9	0	9	8	8	8	10	7	0	2	

Table 4: First five optimal configurations based on the condition number of the FIM.

	P13	T13	P26	T26	NLP	NHP	P3	T3	P49	T49	P5	T5	CN
1	√		√		√	√	√	√	√				−1.9882
2	√		√		√	√		√	√	√			−2.0634
3	√		√		√	√		√	√			√	−2.0713
4	√		√		√	√	√		√	√			−2.1533
5	√		√		√	√	√		√			√	−2.1851
	5	0	5	0	5	5	3	3	5	2	0	2	

Table 5: First five optimal configurations based on the trace of the FIM.

	P13	T13	P26	T26	NLP	NHP	P3	T3	P49	T49	P5	T5	Tr
1	√		√		√	√	√		√	√			2.0122
2	√		√		√	√			√	√		√	2.0117
3			√		√	√	√		√	√		√	2.0030
4	√		√		√	√		√	√	√			2.0025
5	√				√	√	√		√	√		√	2.0003
	4	0	4	0	5	5	3	1	5	5	0	3	

According to the information reported in [17], a number of $m = 7$ sensors seem a reasonable choice for contemporary commercial turbofans.

This optimisation problem is of combinatorial nature. Although algorithms are especially dedicated to this kind of problem, the optimal configuration is found here by means of a brute force technique. The figure of merit is computed for every of the 792 (12 choose 7 binomial coefficient) possible combinations. Unit weights have been applied to each component of the FOM ($W_i = 1.0$, $i = 1, 2, 3$).

Table 3 reports the first ten optimal configurations based on the figure of merit defined in (14). The last column on the right gives the value of the figure of merit for each setup. At first sight, the values may appear quite close to each other, but the reader should recall that the figure of merit is defined on a logarithmic scale. The bottom line in the table gives the frequency of each sensor in the first ten best sensor sets. To complete the picture, the first five optimal configurations according to each component of the FOM are given in Tables 4, 5, and 6. The last column in each of these tables is also expressed in a logarithmic scale.

It can be seen that the optimal configuration according to the full FOM (i.e., first line of Table 3) is ranked, respectively, fourth, first, and second according to the condition number, the trace, and the determinant of the FIM. Hence, the combined metric elegantly merges the different objectives of the

Table 6: First five optimal configurations based on the determinant of the FIM.

	P13	T13	P26	T26	NLP	NHP	P3	T3	P49	T49	P5	T5	Det
1	√		√		√	√		√	√	√			−1.3645
2	√		√		√	√	√		√	√			−1.4557
3	√				√	√	√	√	√	√			−1.6269
4	√		√		√	√		√	√			√	−1.6368
5	√		√		√	√	√	√	√				−1.6608
	5	0	4	0	5	5	3	4	5	3	0	1	

Table 7: Selected sensors sets for further investigations.

Set **A**	P13	T13	NLP	NHP	P3	T3	T5
Set **B**	P13	P26	NLP	NHP	P3	P49	T49
Set **C**	P13	P26	NLP	NHP	P3	T3	T49

optimisation problem. Looking at the last line of each table, it can be deduced that T13, T26, and P5 are not good candidate to the optimal instrumentation whatever the metric considered. On the contrary, P13, P26, P49, and the spool speeds appear to be mandatory in the optimised configuration. This point will be discussed in more details subsequently.

As highlighted in [18], installation of an interturbine pressure sensor becomes more difficult on modern engines. Consequently, the search has been carried out a second time by removing P49 from the list of available sensors, leaving a mere 330 configurations to be examined.

The three sensor sets selected for further investigations are presented in Table 7. Set **A** is the standard instrumentation defined in the frame of the OBIDICOTE project and serves as the baseline for comparison, set **B** is the optimal one when considering P49 as available, and set **C** is the optimal one when discarding P49 from the list. Note that the notion of optimality is relative to the metric defined by (14).

Examining Table 7, one first notices that P13, both spool speeds, and P3 are common to the three sensor sets. P13 is indeed required to correctly assess fan performance. Concerning the spool speeds and P3, these sensors are mandatory for control purpose. It is thus a good point that they appear in the optimal sets. Furthermore, spool speeds are generally very accurately measured, which is one of the reasons of their presence in the optimal configurations. Set **B** is characterised by the presence of P49. This sensor is in fact the only one in the list that allows full differentiation of lpt and hpt faults.

It is also of interest to point out that sets **B** and **C** contain, respectively, 4 and 3 pressure sensors out of 7. This is explained by the fact that pressure sensors are more informative about the engine condition than temperature sensors. It may appear strange that lpt exhaust pressure P5 does not appear in the optimal selection. For a mixed-flow engine, this quantity is nonetheless highly correlated with fan outlet pressure P13. So selecting P13 discards P5 and vice versa. It can also be seen that exhaust gas temperature (defined as T49 or T5, depending on the manufacturer) is part of the optimal sensor sets. An EGT sensor is already fitted on every engine as this quantity serves as a global indicator of engine health for the pilot (so-called EGT margin).

Table 8: Considered fault cases.

a	−1% on SW12R	−0.5% on SE12	fan, lpc
	−0.7% on SW2R	−0.4% on SE2	
b	−1% on SE12		
c	−1% on SW26R	−0.7% on SE26	hpc
d	−1% on SE26		
e	−1% on SW26R		
f	+1% on SW42R		hpt
g	−1% on SW42R	−1% on SE42	
h	−1% on SE42		
i	−1% on SE49		lpt
j	−1% on SW49R	−0.4% on SE49	
k	−1% on SW49R		
l	+1% on SW49R	−0.6% on SE49	
m	+1% on A8IMP		nozzle
n	−1% on A8IMP		

3.3. Evaluation of the sensor sets

In order to evaluate the benefits brought by optimal instrumentation, a series of fault cases, taken from [19] and summarised in Table 8, are considered. They are intended to represent degradations that can be expected on modern turbofans for all individual components. Considered faults involve single as well as multiple health parameters. In the present application, faults have a constant magnitude. Snapshot data are simulated by means of the engine performance model. Gaussian noise, whose magnitude is specified in Table 2, is added to the generated measurements to make them closer to test data.

A diagnosis tool based on a Kalman filter (see [20] for further details) processes the data. Given its stochastic nature, each test case is run twenty times with different realisation of measurement noise. Table 9 reports the averaged results in a very synthetic way. Identification of the fault is declared successful if the estimation error lies within its bounds (see [21] for more details) and is indicated by a check mark (√) in the table.

Table 9: Fault identification results with the 3 sensor sets.

Fault case	**a**	**b**	**c**	**d**	**e**	**f**	**g**	**h**	**i**	**j**	**k**	**l**	**m**	**n**
Set **A**	√	√	√	√	√	√	√	√	√	×	×	×	√	√
Set **B**	√	√	√	√	√	√	√	√	√	√	√	√	×	√
Set **C**	√	√	√	√	√	√	√	√	√	×	√	√	×	√

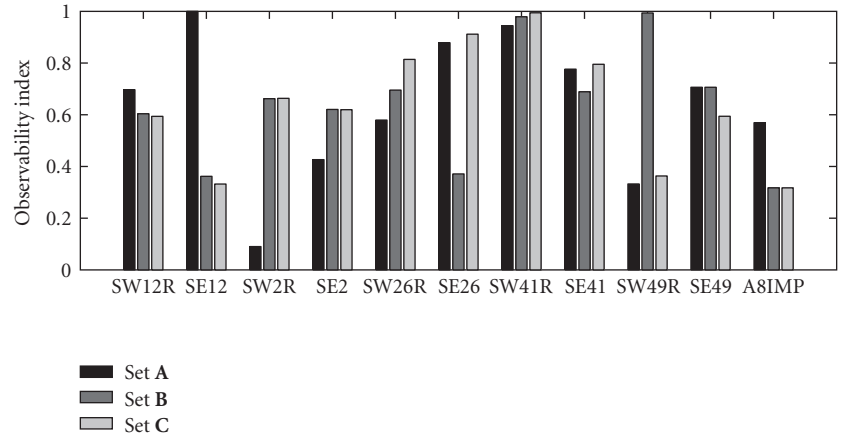

Figure 3: Comparison of the observability indices OI.

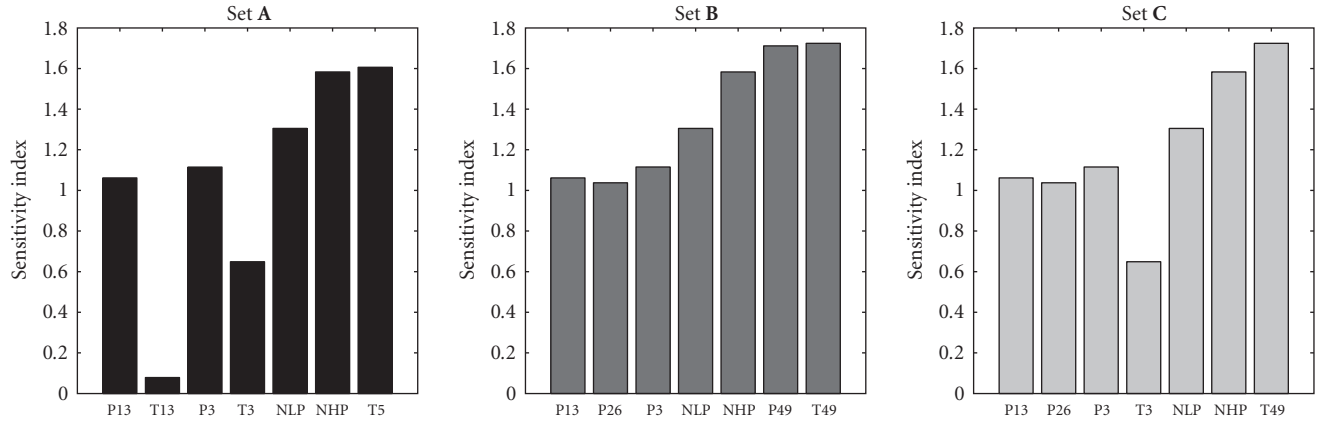

Figure 4: Comparison of the sensitivity indices SI.

The standard instrumentation, set **A**, performs already quite well. It can however be seen that it fails in diagnosing correctly most of the lpt faults (cases **j**, **k**, and **l**). Sensor set **B**, featuring the interturbine pressure sensor, resolves this issue, as previously mentioned. However, fault case **m** is now misidentified. The increase in exhaust nozzle area is confounded with a fan fault. Finally, set **C** achieves some improvement with respect to set **A** too. Most of the lpt faults but case **j** are correctly assessed. As for set **B**, the diagnosis tool is misled by fault case **m**.

3.4. Observability analysis of the sensor sets

The study of the optimal sensor sets is concluded by an observability analysis as per the concepts defined in a previous section. Figure 3 depicts the observability indices of the health parameters for the three sensors sets. Concerning set **A**, the observability of most of the parameters is quite good, except for the booster flow factor, SW2R, and the lpt flow factor SW49R. The optimal set **B** improves the observability of those parameters, on the other hand, it degrades the observability of SE12 and SE26 due to the loss, respectively, of T13 and T3. The nozzle area is also affected. Finally, optimal set **C** offers an intermediate solution. With respect to set **A**, the observability of the lpc is improved as well as the one of the core components. As for set **B**, one can notice a decrease in observability for SE12 and A8IMP.

In Figure 4, the sensitivity indices are compared for each sensor set. From the left picture, it can be seen that both temperature sensors in the cold section, namely, T13 and T3, contribute to a lesser extent in set **A**. The center picture, associated to set **B**, illustrates the effect of the optimisation. The distribution of sensitivity indices is more uniform, and values are higher. Finally, the right graph shows

the sensitivity indices for set **C**. Again, the general trend reveals an increase in the average level. T3 has the lowest contribution among all sensors.

4. DISCUSSION

To complete the analysis of the results, some issues that may lead to further developments of the proposed methodology are discussed in the following.

The first question is related to the assumptions on which the proposed approach relies. The metric defined for sensor selection has indeed been derived for a linearised system, around a given operating point and reference health conditions. Yet, the behaviour of the engine is essentially nonlinear. It would be of interest to evaluate the effects of the nonlinearities on the selection process. On the other hand, the method should be extended to multipoint estimation. A solution could consist in computing the metric from a weighted sum of Fisher information matrices derived for various conditions (both operating and health). Another concern is that the current methodology does not take into account preferential directions for some faults (e.g., the efficiencies are not expected to improve over time). This might impact the sensor selection and should hence be integrated within the figure of merit.

The present contribution is dedicated to the selection of the optimal sensor configuration for a given set of health parameters. Variations of this problem could make up another interesting field of research. A first variant consists in the selection of the best sensors to add to an existing set (for instance imposed by control system requirements). A second one is the selection of the subset of the most observable health parameters given a sensor configuration in order to have a square problem ($m = n$). This problem has already been investigated within the scope of thrust estimation in [22]. The reduction is however carried out in a transformed space, so that the health parameters become actually tuners which turn out to be of little interest for diagnostics purpose.

With a redefined metric, problems such as the minimisation of the number of sensors that allow a satisfactory estimation of a given set of parameters could be investigated. A valuable complementary study could consist in the assessment of the modification in the observability properties of the system in case a sensor is removed either to simplify the configuration or because it is faulty.

Finally, the search for the optimal sensor configuration is achieved here by means of a brute force technique. The primary focus of the present paper is indeed the definition of relevant metrics that describe the problem under consideration. An optimisation algorithm fitted to the combinatorial nature of the problem could supersede the brute force technique which rapidly turns prohibitive as far as computational burden is concerned. In this framework, multiobjective optimisation could be considered. This would leave the designer to select the optimal configuration by trading off the metrics a posteriori rather than a priori through the definition of an aggregated figure of merit. Additional features such as cost and reliability of the sensors should be taken into account in the definition of the metric as they are important factors from an industrial standpoint.

5. CONCLUSION

In this contribution, the problem of optimal selection of the sensor configuration for diagnostics has been revisited from the viewpoint of information theory. From sound mathematical arguments, the Fisher information matrix has appeared to be a relevant quantity for the problem of sensor selection. A figure of merit addressing various issues such as sensor noise, negative redundancy, or orthogonality has been defined based on the Fisher information matrix.

The selection of the optimal sensor configuration with respect to the defined metric has been performed by a naive brute force technique. The enhancement brought by the use of an optimal instrumentation has been underlined with the estimation of a series of simulated but still realistic fault cases that may occur on a contemporary turbofan engine.

NOMENCLATURE

$\hat{\cdot}$	Estimated value
$\tilde{\cdot}$	Scaled value
A8IMP	Nozzle exit area (baseline value: 1.4147 m^2)
bl	Baseline conditions
FIM	Fisher information matrix
hpc	High-pressure compressor
hpt	High-pressure turbine
lpc	Low-pressure compressor
lpt	Low-pressure turbine
m	Number of gas path measurements
n	Number of health parameters
N	Rotational speed
Pi	Total pressure at station i
SEi	Efficiency scaler at station i (baseline value: 1.0)
SWiR	Flow capacity scaler at station i (baseline value: 1.0)
Ti	Total temperature at station i
u	Operating point parameters
w	Health parameters
y	Observed measurements
$\boldsymbol{\epsilon}$	Measurement noise vector
σ	Singular value
$\mathcal{N}(\mathbf{m}, \mathbf{C})$	A Gaussian probability distribution with mean **m** and covariance matrix **C**.

REFERENCES

[1] A. J. Volponi, "Foundation of gas path analysis (part i and ii)," in *Gas Turbine Condition Monitoring and Fault Diagnosis*, Von Karman Institute Lecture Series no. 1, Von Karman Institute for Fluid Dynamics, Brussels, Belgium, 2003.

[2] Y. G. Li, "Performance-analysis-based gas turbine diagnostics: a review," *Proceedings of the Institution of Mechanical Engineers A*, vol. 216, no. 5, pp. 363–377, 2002.

[3] Ph. Kaboukos, P. Oikonomou, A. Stamatis, and K. Mathioudakis, "Optimizing diagnostic effectiveness of mixed turbofans by means of adaptive modelling and choice of appropriate monitoring parameters," in *Ageing Mechanisms*

and Control Specialists' Meeting on Life Management Techniques for Ageing Air Vehicles, Manchester, UK, October 2001.

[4] R. Mushini and D. Simon, "On optimization of sensor selection for aircraft gas turbine engines," in *Proceedings of the 18th International Conference on Systems Engineering (ICSEng '05)*, pp. 9–14, Las Vegas, Nev, USA, August 2005.

[5] G. Bechini, G. Ameyugo, L. Marinai, and R. Singh, "Gas path diagnostics: the importance of measurement selection in the monitoring process," in *Proceedings of the 17th International Symposium on Air Breathing Engines (ISABE '05)*, Munich, Germany, September 2005, ISABE-2005-1281.

[6] M. J. Provost, *The use of optimal estimation techniques in the analysis of gas turbines*, Ph.D. thesis, Cranfield University, Cranfield, UK, 1994.

[7] P. H. Kirkegaard and R. Brincker, "On the optimal location of sensors for parametric identification of linear structural systems," *Mechanical Systems and Signal Processing*, vol. 8, no. 6, pp. 639–647, 1994.

[8] F. W. J. van den Berg, H. C. J. Hoefsloot, H. F. M. Boelens, and A. K. Smilde, "Selection of optimal sensor position in a tubular reactor using robust degree of observability criteria," *Chemical Engineering Science*, vol. 55, no. 4, pp. 827–837, 2000.

[9] A. Vande Wouwer, N. Point, S. Porteman, and M. Remy, "Approach to the selection of optimal sensor locations in distributed parameter systems," *Journal of Process Control*, vol. 10, no. 4, pp. 291–300, 2000.

[10] C. Papadimitriou, "Optimal sensor placement methodology for parametric identification of structural systems," *Journal of Sound and Vibration*, vol. 278, no. 4-5, pp. 923–947, 2004.

[11] M. J. Schervish, *Theory of Statistics*, Springer, New York, NY, USA, 1995.

[12] C. R. Rao, *Linear Statistical Inference and Its Applications*, John Wiley & Sons, New York, NY, USA, 1973.

[13] R. G. Brown, "Not just observable, but how observable," in *Proceedings of the National Electronics Conference (NEC '66)*, vol. 22, pp. 709–714, October 1966.

[14] G. Strang, *Linear Algebra and Its Applications*, Brooks Cole, San Anselmo, Calif, USA, 3rd edition, 1988.

[15] E. Castillo, A. J. Conejo, R. E. Pruneda, and C. Solares, "State estimation observability based on the null space of the measurement Jacobian matrix," *IEEE Transactions on Power Systems*, vol. 20, no. 3, pp. 1656–1658, 2005.

[16] A. Stamatis, K. Mathioudakis, J. Ruiz, and B. Curnock, "Real time engine model implementation for adaptive control and performance monitoring of large civil turbofans," in *Proceedings of the ASME Turbo Expo*, New Orleans, La, USA, June 2001, 2001-GT-0362.

[17] L. Jaw and S. Garg, "Propulsion control technology development in the united states (a historical perspective)," Technical Memorandum 2005-213978, NASA, Moffett Field, Calif, USA, 2005.

[18] B. A. Roth, D. L. Doel, and J. J. Cissell, "Probabilistic matching of turbofan performance models to test data," in *Proceedings of the ASME Turbo Expo*, Reno-Tahoe, Nev, USA, June 2005, GT2005-68201.

[19] B. Curnock, "Obidicote project-word package 4: steady-state test cases," Tech. Rep. DNS62433, Rolls-Royce PLc, London, UK, 2000.

[20] P. Dewallef, *Application of the Kalman filter to health monitoring of gas turbine engines: a sequential approach to robust diagnosis*, Ph.D. thesis, University of Liège, Liège, Belgium, 2005.

[21] S. Borguet and O. Léonard, "Coupling principal component analysis and Kalman filter algorithms for on-line aircraft engine diagnostics," in *Proceedings of the 18th International Symposium on Air Breathing Engines (ISABE '07)*, Beijing, China, September 2007, ISABE-2007-1275.

[22] J. S. Litt, "An optimal orthogonal decomposition method for Kalman filter-based turbofan engine thrust estimation," in *Proceedings of the ASME Turbo Expo*, Reno-Tahoe, Nev, USA, June 2005, GT2005-68808.

Advances in Mechanical Engineering

Special Issue on Heat Transfer in Nanofluids

Call for Papers

Heat transfer can be enhanced by employing various techniques and methodologies, such as increasing either the heat transfer surface or the heat transfer coefficient between the fluid and the surface, which allow high heat transfer rates in a small volume. Cooling is one of the most important technical challenges facing many diverse industries, including microelectronics, transportation, solid-state lighting, and manufacturing.

There is, therefore, an urgent need for new and innovative coolants with improved performance. The novel concept of "nanofluids" has been proposed as a route to surpassing the performance of heat transfer fluids currently available. Several investigations have revealed that the thermal conductivity of the fluid containing nanoparticles could be increased by more than 20% for the case of very low nanoparticle concentrations. Nowadays, a fast growth of research activity in this heat transfer area has arisen.

The aim of this special issue is to collect original research articles as well as review articles on the most recent developments and research efforts in this field, with the purpose of providing guidelines for future research directions.

Topics of interest include, but are not limited to:

- Experimental techniques for measuring thermal properties of nanofluids
- Single-phase convection
- Natural and forced convection cooling
- Pool and flow boiling applications
- Nucleate boiling and critical heat flux and post-CHF measurements
- Flow and heat transfer characteristics in the laminar and turbulent regimes
- Modeling of flow and heat transfer behavior of nanoparticles, nanotubes, and nanofluids under equilibrium and nonequilibrium conditions
- Applications including cooling of electronics, vehicles, fuel cells, transformers, nuclear systems, space systems, drilling, lubrication, thermal storage, drag reduction, and biomedical applications

Before submission authors should carefully read over the journal's Author Guidelines, which are located at http://www.hindawi.com/journals/ame/guidelines.html. Authors should follow the Advances in Mechanical Engineering manuscript format described at the journal site http://www.hindawi.com/journals/ame/. Prospective authors should submit an electronic copy of their complete manuscript through the journal Manuscript Tracking System at http://mts.hindawi.com/ according to the following timetable:

Manuscript Due	July 1, 2009
First Round of Reviews	October 1, 2009
Publication Date	January 1, 2010

Lead Guest Editor

Oronzio Manca, Dipartimento di Ingegneria Aerospaziale e Meccanica, Seconda Università degli Studi di Napoli, Viale Beneduce 10, Via Roma 29, Aversa (CE) 81031, Italy; oronzio.manca@unina2.it

Guest Editors

Yogesh Jaluria, School of Engineering, Rutgers, The State University of New Jersey, 98 Brett Road, Piscataway, NJ 08854-8058, USA; jaluria@jove.rutgers.edu

Dimos Poulikakos, Laboratory of Thermodynamics in Emerging Technologies, Institute of Energy Technology, Swiss Federal Institute of Technology, 8092 Zurich, Switzerland; dimos.poulikakos@ethz.ch

Advances in Mechanical Engineering

Special Issue on Computational Stochastic Structural Dynamics

Call for Papers

For safety and reliability reasons, many dynamic engineering systems excited by intensive forces with irregular time histories have to be analyzed and designed by employing statistical concepts. The development of jet and rocket propulsion systems in the 1940's and subsequently the development of commercial jet aeroplanes in the 1950's that introduced a problem of structural vibration are a good example. In the middle of 1950's and early 1960's, the accelerated development of computers and computational techniques, such as the finite-element method, has enabled the designers to provide less conservative designs for more sophisticated and complex structural systems. Since the early 1950's, many national and international conferences as well as symposia have partially or entirely devoted to presenting results in the field of computational stochastic structural dynamics. It is believed that the latter has reached a stage in which a detailed comparison of the various classes of computational techniques and an examination of design issues for large-scale structural systems are warranted.

The goal of this Special Issue is, therefore, to solicit and publish the most recent research and development in the field, with particular focus on applications of various classes of computational techniques, and to design issues of existing as well as future structural dynamic engineering systems.

Topics of interest include, while strictly confined to the field of computational stochastic structural dynamics, but are not limited to:

- Linear mechanical and structural systems under random excitations
- Nonlinear mechanical and structural systems in aerospace, offshore and ocean, earthquake, automotive, bridge, railway and tunnel, and nuclear engineering
- Future mechanical and structural systems in random environments

Before submission, authors should carefully read over the journal's Author Guidelines, which are located at http://www.hindawi.com/journals/ame/guidelines.html. Prospective authors should submit an electronic copy of their complete manuscript through the journal Manuscript Tracking System at http://mts.hindawi.com/, according to the following timetable:

Manuscript Due	August 1, 2009
First Round of Reviews	November 1, 2009
Publication Date	February 1, 2010

Lead Guest Editor

Cho W. Solomon To, Department of Mechanical Engineering, University of Nebraska, N104 Scott Engineering Center, Lincoln, NE 68588, USA; cto2@unl.edu

Guest Editors

Solomon C. Yim, School of Civil and Construction Engineering, Oregon State University, 220 Owen Hall, Corvallis, OR 97331, USA; solomon.yim@oregonstate.edu

Brian Mace, Institute of Sound and Vibration Research, University of Southampton, Southampton SO17 1BJ, UK; brm@isvr.soton.ac.uk

Advances in Mechanical Engineering

Special Issue on
Micro/Nanotransport Phenomena in Renewable Energy and Energy Efficiency

Call for Papers

Energy has become one of the most important issues of our time as a result of serious concerns about climate change, high oil prices, and peak oil. Renewable energy and energy-saving technologies are potentially crucial parts of the ultimate solutions to both energy sustainability and climate change. Although there are plenty of renewable energy sources available, such as solar, wind, geothermal, they each have some drawbacks: being intermittent, low efficiency and high capital cost, which, at present, limits their applicability. Micro- and nanoscale transport phenomena can play critical role in developing technologies to supply clean energy with both low cost and high efficiency. For example, thermoelectric materials (TE) have application in waste heat recovery and solar energy as well as in the construction of compact coolers or even AC if TE merit, or ZT, can reach 3 or higher. However, it is very challenging to create a perfect TE material with easy electron passage and low phonon flow resistance at the same time. Most recently, nanoscale thermoelectric materials with ZTs as high as 1.4 have been reported, which translates to an efficiency of 14%. Another example is the possibility of using sunlight to breakdown water into hydrogen and oxygen by mimicking photosynthesis. To enable efficient artificial photosynthesis, it is necessary to make artificial multiple electron systems. A breakthrough has been made to accept multiple electrons and release them from single-walled carbon nanotubes (SWNTs) and Phthalocyanines (PCs). Using a catalyst is yet another way to make hydrogen gas from water. A cheap inorganic catalyst has been developed to effectively split hydrogen from water by using sunlight. Additionally, the advanced micro- and nanoscale surface treatment technologies and structures are also very important to the improvement of renewable energy producing and end use efficiencies. Advances in micro- and nanoscale transports can play a crucial role in exploiting renewable energy and developing energy saving technologies in the future. These technologies hold the possibility of providing groundbreaking increases in renewable energy process yields, efficiencies, and lower overall costs, but there is still much to be done before industrializing these technologies. This special issue focuses on these challenges and solicits papers in relevant areas, including, but not limited to, the following:

- Particle transport phenomena in renewable energy conversion processes
- Micro/nanoscale engineered materials for energy conversion and storage
- Fluid transport in micro/nanoscale structures for energy producing process and end use
- Multiphysical transport in microporous media
- Systematical optimization of energy efficiency

Before submission authors should carefully read over the journal's Author Guidelines, which are located at http://www.hindawi.com/journals/ame/guidelines.html. Authors should follow the Advances in Mechanical Engineering manuscript format described at the journal site http://www.hindawi.com/journals/ame/. Prospective authors should submit an electronic copy of their complete manuscript through the journal Manuscript Tracking System at http://mts.hindawi.com/ according to the following timetable:

Manuscript Due	July 1, 2009
First Round of Reviews	October 1, 2009
Publication Date	January 1, 2010

Lead Guest Editor

G. P. "Bud" Peterson, Office of the President, 225 North Avenue, NW, Atlanta, GA 30332-0325, USA; bud.peterson@gatech.edu

Guest Editors

Gang Chen, Department of Mechanical Engineering, Massachusetts Institute of Technology, MA 02139, USA; gchen2@mit.edu

Moran Wang, Los Alamos National Laboratory, Los Alamos, NM 87545, USA; mwang@lanl.gov

Chen Li, Department of Mechanical Engineering, University of Colorado, Boulder, CO 80309, USA; lichen.cu@colorado.edu